Journal of Engineering Science and Technology
Vol. 15, No. 4 (2020) 2841 - 2853

EXPONENTIAL REACHING LAW SLIDING MODE CONTROL FOR DUAL ARM ROBOTS

TUNG LAM NGUYEN[1], HONG QUANG NGUYEN[2,*], MINH DUC DUONG[1], KIEN TRUNG NGO[2]

[1]Hanoi University of Science and Technology
No. 1, Dai Co Viet Road, Ha Noi, Vietnam
[2]Thai Nguyen University of Technology
No. 666, 3/2 Street, Thai Nguyen, Vietnam
*Corresponding Author: quang.nguyenhong@tnut.edu.vn

Abstract

A dual-arm robot, with bi-manual manipulation, can operate in a dexterous human-like manner. However, because of nonlinear, imprecise modeling and interactive properties, the control of dual arm robot becomes sophisticated with some limitations. This paper presents the exponential reaching law sliding mode control for a dual arm robot to move an object, not only translation, but also object rotation in a working plane. Using sliding mode control, the problem of imprecise modeling, parametric uncertainties, system robustness can be solved. Furthermore, exponential reaching law is able to deal with chattering reduction and tracking performance problem. The simulations have shown the effectiveness of the proposed control strategy. In addition, the comparisons to traditional sliding mode control strategy verify the performance advantage of sliding mode control with exponential reaching law.

Keywords: Chattering reduction, Dual arm robots, Exponential reaching law, Sliding mode control.

1. Introduction

One of the earliest attempts to dual arm manipulator control can be found in [1] where the author successfully defines task-oriented single arm and task-oriented dual arm manipulability to optimize redundant arm joint configurations. Sarkar et al. [2] proposes the input-output linearization for maintaining contacts between the object and end-effectors. Dividing the assembling task of the two-arm robot into approach and assembly phases, Dauchez and Delebaree [3] suggested a position control with altered reference position and a hybrid force/position control for manipulating a rigid object. Inspired by the robust nature of variable structure control (VSC), Yao et al. [4] employ VSC control endowed with an adaptive mechanism for robust position and force tracking of the dual arm manipulator. The drawback of this study is that the chattering problem raised from VSC is totally ignored. Similarly, VCS based position and force controllers are developed in [5], however the requirement of fully measured outputs including the contact force can be very costly.

Variations of VSC for maneuvering the dual arm manipulator are adopted in [6, 7] where the authors integrate VSC with adaptive laws for coping with parameter uncertainties and un-modeled dynamics. Some other studies on VSC application in robotic control is observed in [8] where the authors employ high order super twisting sliding mode control for manipulator and in [9] where sliding mode is backed with fuzzy logic for enhancing tracking performance of the dual arm robot. Similarly, composite high order supper twisting sliding mode is developed in [10] for a robot arm to attenuate chattering. Inherited from some parallel position and force control strategies,

Chiaverini et al. [11] fill in the gap between theory and practice by implementing the control algorithms in an industrial manipulator. Several experiment-oriented studies on force and position control can be found in [12-15]. Swain and Morris [16] solve various configurations including fixed-base, free-floating and free-flying base space multi-arm manipulators by using inverse dynamics controls with a force compensator. Cheng et al. [17] discussed the control problem of free-floating dual arm manipulators for space applications, extended state observer is used to deal with uncertain parameters. A dual-flexible-arm robot control problem presented in [18], the dynamics of the flexible robot are approximated and converted into a lumped parameters system. Based on the derived system, the authors propose a hybrid force and position control combined with a vibration attenuator. Flexibility in robot systems is considered in [19], the authors develop system and impact dynamics model of a flexible dual arm manipulator, subsequently, a PD controller is formulated to stabilize the system when capturing an object. Flexible arm control based on assumed mode method can be found in [20]. Force and position control in flexible robot without force sensor based on system constraint and predefined trajectories is done in [21].

Other work on flexible robot is addressed in [22]. One of the most challenging problems of robot applications is interacting with unknown environment, to tackle this situation Chiu et al. [23] propose an adaptive control for force and motion tracking in presence of modelling uncertainties, unknown environmental constraint, and external disturbances. Similar to [5], the technique also requires information about joint position, joint velocity, and contact force. Stability and robustness of a neuro-control systemin robot applications are examined in [24], the authors use radial basis function network accompanied with an auxiliary control for a SCARA type robot, the Lyapunov approach is employed to guarantee the stability of the system. Ozawa et al. [25] deploy a control for dual finger robots for load transportation, the approach is validated via a set of experiments. In addition to force and position control, a method of calculating dynamic load-carrying capacity is presented in [13]. Gueaieb et al. [26] propose a control solution for multiple manipulators coupled through a rigid load, the control can deal with the difficulty raised from the uncertain manipulator dynamics and be proven to be computational benefit since it does not require fuzzy inferencing mechanisms. Analogously, a force/position control for a robot with unknown dynamics interacting with environment is designed in [27], the adaptive algorithm is derived via stability criteria.

In the mentioned researches, the robot moves the object in parallel to x-axis [28]. In order to provide flexible maneuvering ability for the robot, the paper presents a method to manipulate the object in translational and rotational directions. In addition, the exponential reaching time sliding mode control is employed providing faster transient time and lower chattering phenomenon compared to classical sliding mode control. The closed loop dynamics are verified numerically to illustrate the efficiency of the proposed control.

2. Dual arm Robot Dynamics

The system including a dual arm robot handles an object is illustrated in Fig. 1.

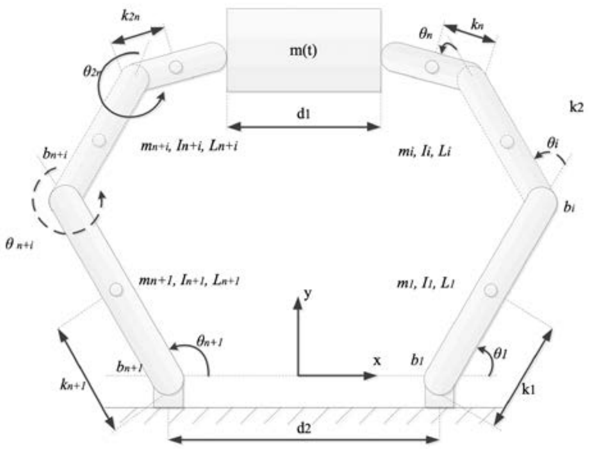

Fig. 1. Physical model of the dual arm robot [9].

The dual arm robot consists of two 2DoF planar robot arms with revolute joints. Different from [9], in this paper, the object can be rotated. In this physical model of the system, m_i, I_i, and $L_i (i=1,2,3,4)$ presents the mass, mass moment of inertia and length of the corresponding links, respectively. In addition, k_i is the distance of the center of mass of each link to the preceding joint and θ_i is the joint angle of the related links. Moreover, $m(t)$ is the mass of the load, d_1 and d_2 denote the width of the rectangle load and the distance between the bases of the two robot arms. In this model, we also consider the viscous in the joints of both robot arms and denoted by b_i . The robot operates in the xy-plane and gravity acts in the negative z-direction.

Because the dual arm robot handles an object, it is vital to consider the interaction between the robot arms and the object. As shown in Fig. 2, the robot arms apply forces F_1, F_2 from the arm tips to the load at position (x_1, y_1) and (x_2, y_2), respectively. The object's center is at (x_m, y_m) and it is rotated about φ_5 around z-axis. The friction forces F_{s1xy}, F_{s2xy} are between the arm tips and the load surface in xy-plane. The friction forces F_{s1z}, F_{s2z} are between the arm ends and the object surface along z axis.

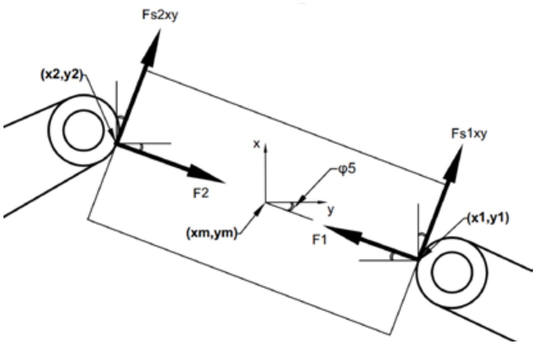

Fig. 2. System coordinate.

Because the system is considered in the xy-plane, it can be supposed that

$$F_{s1z} = F_{s2z} = \frac{m(t)g}{2} \tag{1}$$

where g is gravitational acceleration. Using robot forward kinematics for two robot arms, the positions of arm tips can be calculated as follows

$$x_1 = \frac{d_2}{2} + L_1 \cos\theta_1 + L_2 \cos(\theta_1 + \theta_2) \tag{2}$$

$$y_1 = L_1 sin\theta_1 + L_2 sin(\theta_1 + \theta_2) \tag{3}$$

$$x_2 = -\frac{d_2}{2} + L_1 \cos\theta_3 + L_2 \cos(\theta_3 + \theta_4) \tag{4}$$

$$y_1 = L_1 \sin\theta_3 + L_2 \sin(\theta_3 + \theta_4) \tag{5}$$

Then the relation between object's position and robot tips are

$$\begin{aligned} x_m &= \frac{d_2}{2} + L_1 \cos\theta_1 + L_2 \cos(\theta_1 + \theta_2) - \frac{d_1}{2} cos\varphi_5 \\ &= -\frac{d_2}{2} + L_3 \cos\theta_3 + L_4 \cos(\theta_3 + \theta_4) + \frac{d_1}{2} cos\varphi_5 \end{aligned} \tag{6}$$

$$y_m = L_1 \sin\theta_1 + L_2 \sin(\theta_1+\theta_2) - \frac{d_1}{2}\sin\varphi_5$$
$$= L_3 \sin\theta_3 + L_4 \sin(\theta_3+\theta_4) + \frac{d_1}{2}\sin\varphi_5 \tag{7}$$

The interaction forces between the dual arm robot and the object in the xy-plane are $F_1, F_2, F_{s1xy}, F_{s2xy}$. Therefore, the dynamic equations of the object are:

$$m\ddot{x}_m = -F_1\cos\varphi_5 + F_2\cos\varphi_5 - F_{s1xy}\sin\varphi_5 - F_{s2xy} sin\varphi_5 \tag{8}$$

$$m\ddot{y}_m = -F_1\sin\varphi_5 + F_2\sin\varphi_5 + F_{s1xy}\cos\varphi_5 + F_{s2xy}\cos\varphi_5 \tag{9}$$

$$J\ddot{\varphi}_5 = (F_{s1xy} - F_{s2xy})\frac{d_1}{2} \tag{10}$$

Remark: The object rotation is given in Eq. (10) provide a flexible manipulation ability compared to other works where only translational motion is considered.

From Eqs. (8) and (9) it can be shown that

$$m(\ddot{x}_m\sin\varphi_5 - \ddot{y}_m\cos\varphi_5) = -\sin^2\varphi_5(F_{s1xy}+F_{s2xy}) - \cos^2\varphi_5(F_{s1xy}+F_{s2xy}) \tag{11}$$

or

$$F_{s1xy} + F_{s2xy} = m(\ddot{x}_m\sin\varphi_5 - \ddot{y}_m\cos\varphi_5) \tag{12}$$

Combine with Eq. (10), friction forces F_{s1xy} and F_{s2xy} can be calculated as follows:

$$F_{s1xy} = [m(\ddot{x}_m\sin\varphi_5 - \ddot{y}_m\cos\varphi_5) + \frac{2J\ddot{\varphi}_5}{d_1}] \tag{13}$$

$$F_{s2xy} = [m(\ddot{x}_m\sin\varphi_5 - \ddot{y}_m\cos\varphi_5) - \frac{2J\ddot{\varphi}_5}{d_1}] \tag{14}$$

Substituting Eqs. (13) and (14) into Eq. (8) results in;

$$\Delta F = F_2 - F_1 = m\frac{(1+\sin^2\varphi_5)\ddot{x}_m + \sin\varphi_5\cos\varphi_5\ddot{y}_m}{\cos\varphi_5} \tag{15}$$

In order to handle the object effectively, the following conditions must be obtained:

$$F_{s1xy}^2 + F_{s1z}^2 \le (\mu F_1)^2, F_{s2xy}^2 + F_{s2z}^2 \le (\mu F_2)^2 \tag{16}$$

where μ is dry friction coefficient of the object. Since the direction of acting forces F_1 and F_2 are always direct towards the object, the friction force equation that provides a positive signed solution for both F_1 and F_2 should be selected. Therefore, we have to consider two situations corresponding the relation between F_1 and F_2. In the first situation, if $F_2 > F_1$ (i.e. $\Delta F > 0$), using Eq. (16) F_1 and F_2 can be calculated as following:

$$F_1 = \frac{1}{\mu}\sqrt{F_{s1xy}^2 + F_{s1z}^2}, \quad F_2 = F_1 + \Delta F \tag{17}$$

where F_{s1xy}, F_{s1z}, and ΔF are calculated using Eqs. (13), (1) and (15) respectively. In the second situation, if $F_2 \le F_1$ (i.e. $\Delta F \le 0$), using Eq. (16) with the analogous approach, F_1 and F_2 can be calculated as following:

$$F_2 = \frac{1}{\mu}\sqrt{F_{s2xy}^2 + F_{s2z}^2}, \quad F_1 = F_2 - \Delta F \tag{18}$$

where F_{s2xy}, F_{s2z}, and ΔF are calculated using Eqs. (14), (1), and (15) respectively. The dual arm robot system includes two 2DoF robot arms that handles and the object can be considered as two separated robot arm with external forces F_1, F_{s1xy} for the first arm and F_2, F_{s2xy} for the second arm. Therefore, the governing equations for the dual arm robot system are as following:

$$M(\overline{\mathbf{q}})\ddot{\overline{\mathbf{q}}} + C(\overline{\mathbf{q}}, \dot{\overline{\mathbf{q}}}) = \overline{\boldsymbol{\tau}} + J(\overline{\mathbf{q}})^T \overline{F} - \boldsymbol{\beta}\dot{\overline{\mathbf{q}}} + \overline{\mathbf{w}} \tag{19}$$

where $\overline{\mathbf{q}} = [\theta_1, \theta_2, \theta_3, \theta_4]^T$ is angular vector, $\overline{\boldsymbol{\tau}} = [\tau_1, \tau_2, \tau_3, \tau_4]^T$ is torque input vector, $\overline{\mathbf{F}} = [F_{1x}, F_{1y}, F_{2x}, F_{2y}]^T$ is external force vector, $\overline{\omega} = [\omega_1, \omega_2, \omega_3, \omega_4]^T$ is external disturbance torque vector.

The external force component can be calculated from F_1, F_{s1xy}, F_2, and F_{s2xy} as following:

$$F_{1x} = F_1 \cos\varphi_5 + F_{s1xy}\sin\varphi_5, \quad F_{1y} = F\sin\varphi_5 - F_{s1xy}\cos\varphi_5 \tag{20}$$

$$F_{2x} = -F_2 \cos\varphi_5 + F_{s2xy}\sin\varphi_5, \quad F_{2y} = -F_2\sin\varphi_5 - F_{s2xy}\cos\varphi_5 \tag{21}$$

In addition, $\mathbf{M}(\overline{\mathbf{q}})$ is inertia matrix, $\mathbf{C}(\overline{\mathbf{q}}, \dot{\overline{\mathbf{q}}})$ is Coriolis matrix, $\mathbf{J}(\overline{\mathbf{q}})$ is Jacobian matrix, β is viscous friction matrix, and they are calculated as following:

$$\mathbf{M}(\overline{\mathbf{q}}) = \begin{bmatrix} A_1 + A_2 + 2A_3\cos\theta_2 & A_2 + A_3\cos\theta_2 & 0 & 0 \\ A_2 + A_3\cos\theta_2 & A_2 & 0 & 0 \\ 0 & 0 & A_4 + A_5 + 2A_6\cos\theta_4 & A_5 + A_6\cos\theta_4 \\ 0 & 0 & A_5 + A_6\cos\theta_4 & A_5 \end{bmatrix};$$

$$\mathbf{C}(\overline{\mathbf{q}}, \dot{\overline{\mathbf{q}}}) = \begin{bmatrix} -A_3\sin\theta_2(\dot{\theta}_2^2 + 2\dot{\theta}_1\dot{\theta}_2) \\ -A_3\dot{\theta}_1\dot{\theta}_2\sin\theta_2 \\ -A_6\sin\theta_4(\dot{\theta}_4^2 + 2\dot{\theta}_3\dot{\theta}_4) \\ -A_6\dot{\theta}_3\dot{\theta}_4\sin\theta_4 \end{bmatrix}; \ \boldsymbol{\beta} = \begin{bmatrix} b_1 & 0 & 0 & 0 \\ 0 & b_2 & 0 & 0 \\ 0 & 0 & b_3 & 0 \\ 0 & 0 & 0 & b_4 \end{bmatrix};$$

$$\mathbf{J}(\overline{\mathbf{q}}) = \begin{bmatrix} -L_1\sin\theta_1 - L_2\sin(\theta_1+\theta_2) & -L_2\sin(\theta_1+\theta_2) & 0 & 0 \\ L_1\cos\theta_1 + L_2\cos(\theta_1+\theta_2) & L_2\cos(\theta_1+\theta_2) & 0 & 0 \\ 0 & 0 & -L_3\sin\theta_3 - L_4\sin(\theta_3+\theta_4) & -L_4\sin(\theta_3+\theta_4) \\ 0 & 0 & L_3\cos\theta_3 + L_4\cos(\theta_3+\theta_4) & L_4\cos(\theta_3+\theta_4) \end{bmatrix};$$

where $\mathrm{A_j}\,(j = 1, 2, \ldots, 6)$ are the constant coefficients given by

$$A_1 = m_1k_1^2 + m_2L_1^2 + I_1 \qquad A_2 = m_2k_2^2 + I_2 \qquad A_3 = m_2L_1k_2 \tag{22}$$

$$A_4 = m_3k_3^2 + m_4L_3^2 + I_3 \qquad A_5 = m_4k_4^2 + I_4 \qquad A_6 = m_4L_3k_4 \tag{23}$$

3. Sliding Mode Control with Exponential Reaching Law

In order to design the sliding mode controller with exponential reaching law for dual arm robot, the dynamic equations are rewritten under first order system as following

$$\dot{\mathbf{x}} = \mathbf{f}(\mathbf{x},t) + \mathbf{B}(\mathbf{x},t)\mathbf{u}, \tag{24}$$

where

$\mathbf{x} = [\overline{\mathbf{q}}; \dot{\overline{\mathbf{q}}}] = [\theta_1\ \theta_2\ \theta_3\ \theta_4\ \dot{\theta}_1\ \dot{\theta}_2\ \dot{\theta}_3\ \dot{\theta}_4]^T$ is system state vector;

$\mathbf{u} = [O_{4\times 1}; \overline{\tau}] = [0\,0\,0\,0\,\tau_1\ \tau_2\ \tau_3\ \tau_4]^T$ is control input vector; $\mathbf{B}(\mathbf{x},t) = [O_{4\times 4}; M(\overline{q})^{-1}]$;

$\mathbf{f}(\mathbf{x},t) = [\dot{\overline{\mathbf{q}}}; \overline{\mathbf{f}}]$ with $\overline{\mathbf{f}} = \mathbf{M}(\overline{\mathbf{q}})^{-1}(\mathbf{J}^T\overline{\mathbf{F}} - \overline{\boldsymbol{\beta}} - \mathbf{C}(\overline{\mathbf{q}}, \dot{\overline{\mathbf{q}}}))$.

The control problem is to drive the manipulator joints to desired value. Toward this end, the sliding surface is selected as follows

$$\mathbf{s}(x) = [s_1(x)\ldots s_4(x)\,0\ldots 0]^T = \overline{\mathbf{G}}\Delta\boldsymbol{\theta} \tag{25}$$

where

$\Delta\boldsymbol{\theta} = \mathbf{x}_r - \mathbf{x} = [\mathbf{e}, \dot{\mathbf{e}}]^T$ is the system error, and

$$\mathbf{G} = \begin{bmatrix} \lambda_1 & 0 & 0 & 0 & 1 & 0 & 0 & 0 \\ 0 & \lambda_2 & 0 & 0 & 0 & 1 & 0 & 0 \\ 0 & 0 & \lambda_3 & 0 & 0 & 0 & 1 & 0 \\ 0 & 0 & 0 & \lambda_4 & 0 & 0 & 0 & 1 \end{bmatrix};$$ $\lambda_i\,(i = 1,..,4)$ is sliding surface coefficient.

Input **u** is designed such as the system goes to the sliding surface and then stay there. Therefore, input **u** is divided into two parts as follows:

$$\mathbf{u} = \begin{cases} \mathbf{u}_{eq}, \mathbf{s}(x) = 0 \\ \mathbf{u}_N, \mathbf{s}(x) \neq 0 \end{cases} \tag{26}$$

Control signal $\mathbf{u}_{eq}$ keeps the system in the sliding surface, then it has to satisfy $d\mathbf{s}/dt = 0$, it means

$$\dot{\mathbf{s}} = \overline{\mathbf{G}}\,\dot{\mathbf{x}}_r - \overline{\mathbf{G}}\,\dot{\mathbf{x}} = \overline{\mathbf{G}}\,\dot{\mathbf{x}}_r - \overline{\mathbf{G}}(\mathbf{f}(\mathbf{x},t) + \mathbf{B}(\mathbf{x},t)\mathbf{u}_{eq}) = 0 \tag{27}$$

where $\dot{s} = [\dot{s}_1 \ldots \dot{s}_4\ 0\ldots 0]^T$. Then, $\mathbf{u}_{eq} = [\overline{\mathbf{G}}\mathbf{B}(\mathbf{x},t)]^{-1}[\overline{\mathbf{G}}\,\dot{\mathbf{x}}_r - \overline{\mathbf{G}}\mathbf{f}(\mathbf{x},t)]$ (28)

Control signal u_N keeps the system to the sliding surface. In this paper, sliding mode control with exponential reaching law [28] is applied, sliding surface is chosen as

$$\dot{\mathbf{s}} = -\frac{k_i}{N_i(s_i)}\mathrm{sign}(\mathbf{s}), k_i > 0 \tag{29}$$

where we have used $\text{sign}(\mathbf{s}) = [\text{sign}(s_1)\ldots\text{sign}(s_4)\,0\ldots0]^T$ and

$$N_i(s_i) = \delta_i + (1-\boldsymbol{\delta}_i)e^{-\alpha_i|s_i|^{p_i}} \tag{30}$$

in which δ_i is a strictly positive constant that is less than one, p_i is a strictly positive integer, and α_i where $i = 1\ldots4$ is also strictly positive. It should be noted that the difference between exponential reaching law and conventional sliding mode control is the varying coefficient, $\frac{k}{N_i(s_i)}$ surges in reaching mode proving fast approaching time and reduces to k in sliding phase hence lowering chattering effect. If δ_i is set to one, exponential reaching time sliding mode becomes the conventional one. Thus, it is straightforward to show that

$$\dot{\mathbf{s}} = \overline{\mathbf{G}}\,\dot{\mathbf{x}}_r - \overline{\mathbf{G}}(\mathbf{f}(\mathbf{x},t) + \mathbf{B}(\mathbf{x},t)\mathbf{u}_N) = -\frac{k_i}{N_i(s_i)}\text{sign}(\mathbf{s}) \tag{31}$$

Then it is straightforward to show that

$$\mathbf{u}_N = [\overline{\mathbf{G}}\mathbf{B}(\mathbf{x},t)]^{-1}[\overline{\mathbf{G}}\dot{x}_r - \overline{\mathbf{G}}\mathbf{f}(\mathbf{x},t) + \frac{k_i}{N_i(s_i)}\text{sign}(\mathbf{s})] \tag{32}$$

4. Result and Discussion

In order to justify the effectiveness of the designed control method, numerical simulations of dual arm robot with both conventional sliding mode control and sliding mode control with exponential reaching law are performed. The robot parameters are given as in Table 1.

Table 1. The dual arm robot parameters.

m_1 = 5 kg	m_2 = 4 kg	m_3 = 4 kg	m_4 = 4 kg
L_1 = 0.5 m	L_2 = 0.4 m	L_3 = 0.5 m	L_4 = 0.4 m
k_1 = 0.25 m	k_2 = 0.2 m	k_3 = 0.25 m	k_4 = 0.4 m
I_1 = 0.1 kgm^2	I_2 = 0.08 kgm^2	I_3 = 0.1 kgm^2	I_4 = 0.08 kgm^2
b_1 = 100 Nms	b_2 = 100 Nms	b_3 = 100 Nms	b_4 = 100 Nms
m_{load} = 56 kg	μ = 0.3	d_1= 0.2 m	d_2=0.4 m

It is noted that indexes 1, 2, 3, and 4 are defined according to Fig.1. The simulation scenario is as following. The initial of dual robot's joint angle is $\theta = [0 \;\; \pi/2 \;\; -\pi/2]^T$. Then, the initial position of the first and the second arm's tips are [0.7; 0.4] and [-0.7;0.4]. The object first is a rectangle with the center point is placed at [-0.2 0.7]. At the first stage, in order to grasp the object, the first arm's tip will move to [-0.1 0.7] and the second arm's tip will move to [-0.3 0.7]. Then, at the second stage, the dual arm robot will move the object's center point to [0 0.4] without rotate the object. And finally, at the third stage, the dual arm robot will move the object's center point to [0.4 0] while rotate the object about 90 degree. In order to move the dual arm robot according to the above scenario, the trajectories of two robot arm's tips are designed as following. At the first stage (in the first 2 seconds), the trajectories are

$$x_{1r} = -0.1 + 0.8e^{-5t^3} \qquad x_{2r} = -0.3 - 0.4e^{-5t^3}$$
$$y_{1r} = 0.7 - 0.3e^{-5t^3} \qquad y_{2r} = 0.7 - 0.3e^{-5t^3} \tag{33}$$

At the second stage (in next 2 seconds), the trajectories are

$$x_{1r} = 0.1 - 0.2e^{-5(t-2)^3} \qquad x_{2r} = -0.1 - 0.2e^{-5(t-2)^3}$$
$$y_{1r} = 0.4 - 0.3e^{-5(t-2)^3} \qquad y_{2r} = 0.4 - 0.3e^{-5(t-2)^3}$$

At the third stage (in the last 2 seconds), the trajectories of the object are

$$x_m = 0.4 - 0.4e^{-5(t-4)^3}, \quad y_m = 0.4e^{-5(t-2)^3}, \quad \varphi_{5r} = \frac{-\pi}{2} + \frac{-\pi}{2}e^{-5(t-4)^3} \tag{34}$$

Then the trajectories of dual arm robot are

$$x_{1r} = x_m + \frac{d_1}{2}cos\varphi_{r5} \qquad x_{2r} = x_m - \frac{d_1}{2}cos\varphi_{r5}$$
$$y_{1r} = y_m + \frac{d_1}{2}sin\varphi_{r5} \qquad y_{2r} = y_m - \frac{d_1}{2}sin\varphi_{r5} \tag{35}$$

The control parameters for exponential reaching law SMC are $\alpha = [10\ \ 10\ \ 10\ \ 10]^T$, $\delta = [1\ 1\ 1\ 1]^T$, $k = [500\ \ 500\ \ 500\ \ 500]^T$, and $p = [1\ 1\ 1\ 1]^T$. It is assumed that the robot is subjected to periodic external disturbances of $\varpi = 2[\sin 10\pi t\ \ \sin 10\pi t\ \ -\sin 10\pi t\ \ -\sin 10\pi t]^T$.

The joint and object tracking angle errors illustrated in Figs. 3 and 4 clearly show the advantage of exponential reaching law sliding mode control over the conventional one, especially when the robot start to rotate the object (at 4th second). Fig. 5 show considerable object tracking error of the conventional sliding mode control. In addition, the property of limiting chattering in control input can be observed in Figs. 6 and 7, conventional sliding mode control produces high switching pattern in input torque, this leads to difficulties in practical applications.

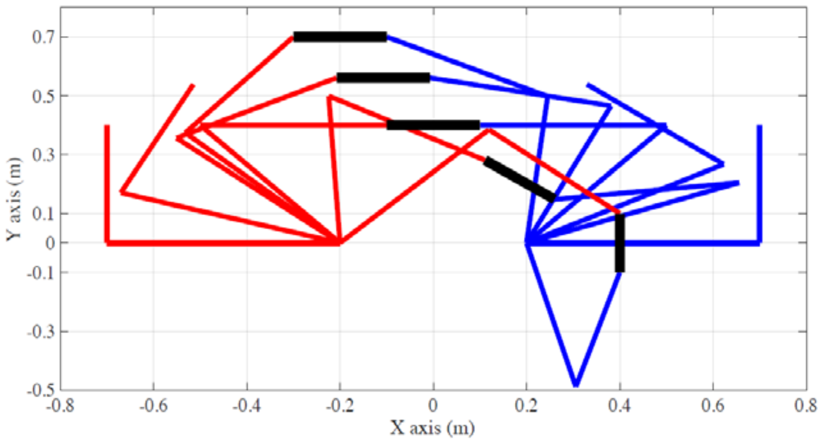

Fig. 3. Robot motion.

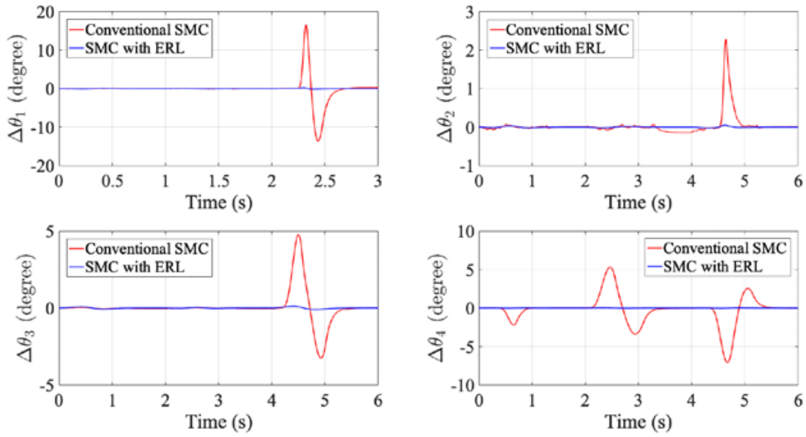

Fig. 4. Joint angle tracking errors.

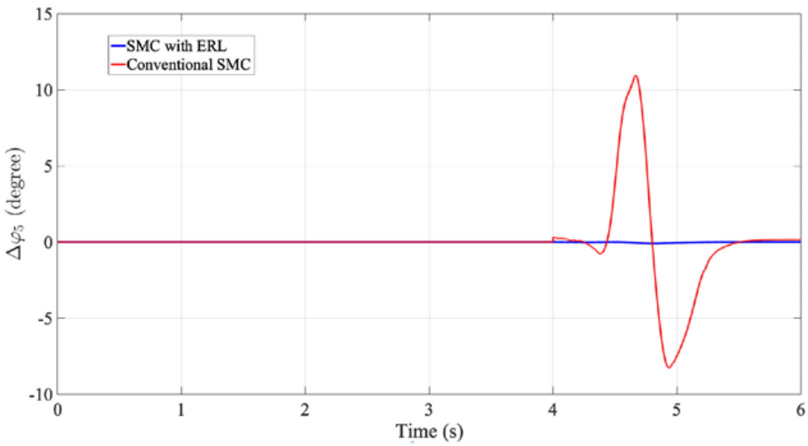

Fig. 5. Object tracking angle error.

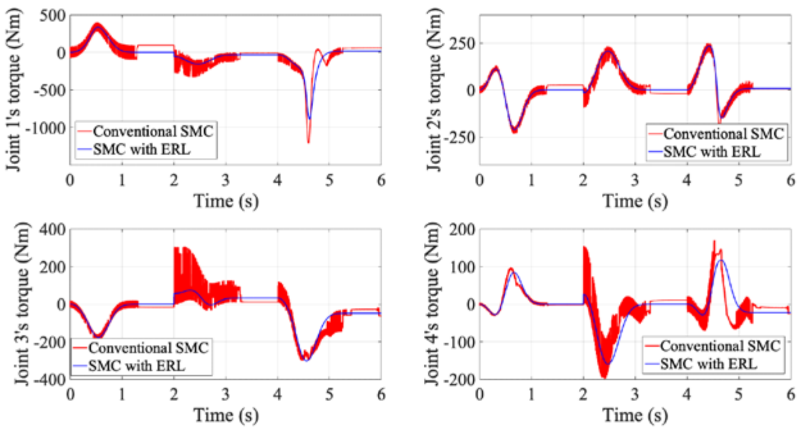

Fig. 6. Input torques.

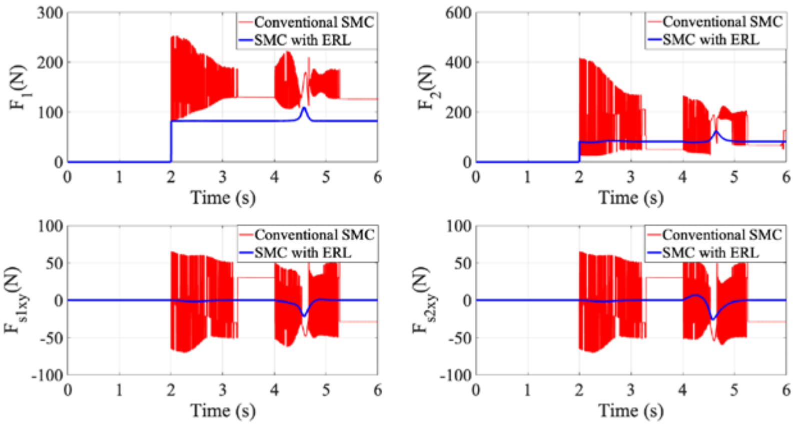

Fig. 7. Contact forces.

5. Conclusions

Dynamics formulation and control design problem of the dual arm robot is addressed in the paper. Dissimilar to other works, the robot considered in the paper can relocate and rotate the object simultaneously. Toward the goal of archiving fast dynamical transient response and system robustness, the exponential reaching law sliding mode control is designed for the dual arm manipulator. In comparison with conventional sliding mode control, the modified version with exponential reaching provide better transient performance and lower tracking error. In addition, due to the existence of exponential term, chattering phenomenon is considerably reduced. Numerical simulations are provided to illustrate the concluding remarks. The future work of the research will involve the robot dynamics in three-dimensional space.

Acknowledgements

This research was funded by Thai Nguyen University of Technology, No. 666, 3/2 Street, Thai Nguyen, Viet Nam.

References

1. Lee, S. (1989). Dual redundant arm configuration optimization with task-oriented dual arm manipulability. *IEEE Transactions on Robotics and Automation*, 5(1), 78-97.
2. Sarkar, N.; Yun, X.; and Kumar, V. (1987). Dynamic control of 3-D rolling contacts in two-arm manipulation. *IEEE Transactions on Robotics and Automation*, 13(3), 364-376.
3. Dauchez, P. and Delebarre, X. (1991). Force-controlled assembly of two objects with a two-arm robot. *Robotica*, 9(3), 299-306.
4. Yao, B.; Chan, S.P.; and Wang, D. (1994). Variable structure adaptive motion and force control of robot manipulators. *Automatica*, 30(9), 1473-1477.
5. Parra-Vega, V.; and Arimoto, S. (1996). A passivity-based adaptive sliding mode position-force control for robot manipulators. *International Journal of Adaptive Control Signal Processing*, 10(4-5), 365-377.

6. Tuan, L.A.; Joo, Y.H.; Duong, P. X.; and Tien, L.Q. (2017). Parameter estimator integrated-sliding mode control of dual arm robots. *International Journal of Control, Automation and Systems*, 15(6), 2754-2763.
7. Tuan, L.A.; Joo, Y.H.; Tien, L.Q.; and Duong, P.X. (2017). Adaptive neural network second order sliding mode control of dual arm robots. *International Journal of Control, Automation and Systems*, 15(6), 1-9.
8. Tayebi-Haghighi, S.; Piltan, F.; and Kim, J.M. (2018). Robust Composite high-order super-twisting sliding mode control of robot manipulators. *Robotics*, 7(1), 13.
9. Hacioglu, Y.; Arslan, Y.Z.; and Yagiz, N. (2011). MIMO fuzzy sliding mode controlled dual arm robot in load transportation. *Journal of The Franklin Institute*, 348(8), 1886-1902.
10. Tayebi-Haghighi, S.; Piltan, F.; Kim, J.-M. (2018). Robust composite high-order super-twisting sliding mode control of robot manipulators. *Robotics*, 7(1), 13, 1-18.
11. Chiaverini, S.I.; Siciliano, B.; and Villani, L. (1996). Parallel force and position control schemes with experiments on an industrial robot manipulator. *IFAC Proceedings*, 29(1), 25-30.
12. Natale, C.; Siciliano, B.; and Villani, L. (1999). Robust hybrid force/position control with experiments on an industrial robot. *IEEE/ASME International Conference on Advanced Intelligent Mechatronics*, no. 5, 956-960.
13. Tinós, R.; Terra, M.H.; and Ishihara, J.Y. (2006). Motion and force control of cooperative robotic manipulators with passive joints. *IEEE Transactions on Control Systems Technology*, 14(4), 725-734.
14. Gudiño-Lau, J.; and Arteaga, M.A. (2005). Dynamic model and simulation of cooperative robots: A case study. *Robotica*, 23(5), 615-624.
15. Sijs, J.; Liefhebber, F.; and Romer, G.W.R. (2007). Combined Position and Force Control for a robotic manipulator. *10th International Conference of Rehabilitation Robotics*, 106-111.
16. Swain, A.K.; and Morris, A.S. (2004). Dynamic control of multi-arm co-operating manipulator systems. *Robotica*, 22(3), 271-283.
17. Cheng, J.; and Chen, L. (2017). Coordinated robust control based on extended state observer of dual-arm space robot with closed chain for transferring a target. *Proceedings of the Institution of Mechanical Engineers, Part G: Journal of Aerospace Engineering*, 232(13), 2489-2498.
18. Yamano, M.; Kim, J.S.; Konno, A.; and Uchiyama, M. (2004). Cooperative control of a 3D dual-flexible-arm robot. *Journal of Intelligent and Robotic Systems: Theory and Applications*, 39(1), 1-15.
19. Liu, S.; Wu, L.; and Lu, Z. (2007). Impact dynamics and control of a flexible dual-arm space robot capturing an object. *Applied Mathematics and Computaions*, 185(2), 1149-1159.
20. Licheng, W.; Fuchun, S.; Zengqi, S.; and Wenjing, S. (2002). Dynamic Modeling, Control and Simulation of Flexible Dual-Arm Space Robot. *2002 IEEE Region 10 Conference on Computers, Communications, Control and Power Engineering*, 1282-1285.

21. Nicolis, D.; Zanchettin, A.M.; and Rocco, P. (2016). Constraint-Based and Sensorless Force Control with an Application to a Lightweight Dual-Arm Robot. *IEEE Robotics and Automation Letters.*, 1(1), 340-347.
22. Kruger, J.; Schreck, G.; and Surdilovic, D. (2011), Dual arm robot for flexible and cooperative assembly. *CIRP Annals-Manufacturing Technology*, 60(1), 5-8.
23. Chiu, C.; Lian, K.; and Wu, T. (2004). Robust adaptive motion/force tracking control design for uncertain constrained robot manipulators. *Automatika*, 40(12), 2111-2119.
24. Lee, M.J.; and Choi, Y.K. (2004). An adaptive neurocontroller using RBFN for robot manipulators. *IEEE Transactions on Industrial Electronics.*, 51(3), 711-717.
25. Ozawa, R.; Arimoto, S.; Nakamura, S.; and Bae, J.H. (2005). Control of an object with parallel surfaces by a pair of finger robots without object sensing. *IEEE Transactions on Robotics*, 21(5), 965-976.
26. Gueaieb, W.; Al-Sharhan, S.; and Bolic, M. (2007). Robust computationally efficient control of cooperative closed-chain manipulators with uncertain dynamics. *Automatica*, 43(5), 842-851.
27. Kouya, D.N.; Saad, M.; and Okou, F.A. (2011). A novel adaptive hybrid force-position control of a robotic manipulator. *International Journal of Modelling, Identification and Control*, 13(1), 97-107.
28. Fallaha, C.; Saad, M.; Kanaan, H.Y.; and Al-Haddad, K. (2011). Sliding mode robot control with exponential reaching law. *IEEE Transaction on Industrial Electronics*, 58(2), 600-610.